



## OPEN ACCESS

## EDITED BY

Sanjay M. R.,  
King Mongkut's University of Technology  
North Bangkok, Thailand

## REVIEWED BY

Vishwas Mahesh,  
Siddaganga Institute of Technology,  
Tumakuru, India  
Madhu Puttegowda,  
Malnad College of Engineering, India

## \*CORRESPONDENCE

Seshathiri Dhanasekaran,  
✉ seshathiri.dhanasekaran@uit.no

RECEIVED 26 July 2023

ACCEPTED 30 October 2023

PUBLISHED 24 November 2023

## CITATION

Natrayan L, Janardhan G, Paramasivam P and Dhanasekaran S (2023), Enhancing mechanical performance of TiO<sub>2</sub> filler with Kevlar/epoxy-based hybrid composites in a cryogenic environment: a statistical optimization study using RSM and ANN methods.

*Front. Mater.* 10:1267514.

doi: 10.3389/fmats.2023.1267514

## COPYRIGHT

© 2023 Natrayan, Janardhan, Paramasivam and Dhanasekaran. This is an open-access article distributed under the terms of the [Creative Commons Attribution License \(CC BY\)](https://creativecommons.org/licenses/by/4.0/). The use, distribution or reproduction in other forums is permitted, provided the original author(s) and the copyright owner(s) are credited and that the original publication in this journal is cited, in accordance with accepted academic practice. No use, distribution or reproduction is permitted which does not comply with these terms.

# Enhancing mechanical performance of TiO<sub>2</sub> filler with Kevlar/epoxy-based hybrid composites in a cryogenic environment: a statistical optimization study using RSM and ANN methods

L. Natrayan<sup>1</sup>, Gorti Janardhan<sup>2</sup>, Prabhu Paramasivam<sup>3</sup> and Seshathiri Dhanasekaran<sup>4\*</sup>

<sup>1</sup>Department of Mechanical Engineering, Saveetha School of Engineering, SIMATS, Chennai, Tamil Nadu, India, <sup>2</sup>Department of Mechanical Engineering, GMR Institute of Technology, Razam, Andhra Pradesh, India, <sup>3</sup>Department of Mechanical Engineering, College of Engineering and Technology, Mattu University, Mettu, Ethiopia, <sup>4</sup>Department of Computer Science, UiT the Arctic University of Norway, Tromsø, Norway

This research aims to investigate the mechanical performance of the different weight proportions of nano-TiO<sub>2</sub> combined with Kevlar fiber-based hybrid composites under cryogenic conditions. The following parameters were thus considered: (i) Kevlar fiber mat type (100 and 200 gsm); (ii) weight proportions of TiO<sub>2</sub> nanofiller (2 and 6 wt%); and (iii) cryogenic processing time (10–30 min at –196°C). The composites were fabricated through compression molding techniques. After fabrication, the mechanical characteristics of the prepared nanocomposites—such as tensile, bending, and impact properties—were evaluated. The optimal mechanical strength of nanofiller-based composites was analyzed using response surface methodology (RSM) and artificial neural networks (ANNs). Compositions, such as four weight percentages of nano-TiO<sub>2</sub> filler, 200 gsm of the Kevlar fiber mat, and 20 min of cryogenic treatment, were shown to produce the maximum mechanical strength (65.47 MPa of tensile, 97.34 MPa of flexural, and 52.82 J/m<sup>2</sup> of impact). This is because residual strains are produced at low temperatures (cryogenic treatment) due to unstable matrices and fiber contraction. This interfacial stress helps maintain a relationship between the reinforcement and resin and improves adhesion, leading to improved results. Based on statistical evaluation, the ratio of correlation ( $R^2$ ), mean square deviation, and average error function of the experimental and validation data sets of the experimental models were analyzed. The ANN displays 0.9864 values for impact, 0.9842 for flexural, and 0.9764 for tensile. ANN and RSM models were used to forecast the mechanical efficiency of the suggested nanocomposites with up to 95% reliability.

## KEYWORDS

nanocomposites, Kevlar mat, response surface methodology, optimization, mechanical properties, sustainability, cryogenic environment

## 1 Introduction

Research interest in the use of natural fiber as reinforcement in composites has grown over the past 15 years to create environmentally friendly, renewable sources. The recyclability, availability, and excellent mechanical properties of natural fabrics are the main reasons for accelerating their use as reinforcement to replace conventional fibers (Luzy et al., 2019; Behnam Hosseini, 2020). Organic fiber-based composite materials have aroused interest because they can replace artificial fiber-based composites. Biosourced fibers can meet industry needs for reinforced composites by 31% (Li et al., 2006; Su et al., 2008). Bast fiber-based (kenaf, hemp, ramie, and jute) composites have brought to attention some natural materials accessible in various industries, including maritime, automobile, and architecture. However, the watery character of organic fiber composites, which affects the interface qualities between reinforcement and resin and reduces the composite's mechanical capabilities, is a major problem (Rana et al., 1998; Li et al., 2000). Textile composites are commonly utilized; these incorporate reinforcement of either natural or synthetic fibers or textiles within the matrix. Composite materials, which are characterized by considerably reduced weight, exhibit enhanced mechanical, thermal, electrical, and ballistic properties. Depending on the application's specific requirements, these attributes can be further fine-tuned with diverse surface treatments (Velmurugan and Babu, 2020). Synthetic fibers constitute the primary constituents; these encompass a range of materials including glass, carbon, boron, polyethylene, and aramid fibers. Among these, para-aramid Kevlar fibers have stood out, featuring 1,4-para-substituted aromatic rings. These monomeric chains form unidirectional hydrogen bonds that combine to generate sheets and are subsequently rolled into microfibrils with diameters of 12–60 nm. When these microfibrils aggregate, they form Kevlar fibers known for their rigidity and nonlinear behavior under crosswise compression and longitudinal elasticity when subjected to longitudinal strain (Thakur et al., 2014). Highly crystalline poly-aramid Kevlar fibers exhibit densities of 1.44–1.47 g per cm<sup>3</sup>. Kevlar fibers come in various grades, including K-29 (maximal hardness), K-49 (greater elasticity), K-100, K-119 (enhanced ductility), K-129 (superior shock resistance), K-149, and KM2 (notable rigidity and toughness). Kevlar fibers are favored as textiles due to their ability to reinforce the polymeric matrix, yielding Kevlar fiber-reinforced polymer (KFRP) textile composites. These composites are renowned for their exceptional durability, elasticity, impact resistance, shock-absorbing capabilities, heat resistance, thermal insulation, low density, minimal thermal conductivity, and heightened multidimensional consistency (Prasob and Sasikumar, 2018; Ganesan et al., 2020). The matrix material in these composites can be thermoset polymers such as epoxy, phenolic, or bismaleimide, known for their exceptional toughness, high heat resistance, and favorable electrical properties. Alternatively, a thermoplastic polymer may be employed, such as low- or high-density polyethylene, polyester, acrylics, or polypropylene (PP). KFRPs find widespread application in creating thermal insulators with stress-bearing rigidity across industries like cryogenics, aerospace, military, and law enforcement protection against high-velocity projectiles and containment systems for propulsion engines (Uma Devi et al., 1997;

Prasob and Sasikumar, 2019). Due to their anisotropic behavior and composition, Kevlar fibers exhibit lower compressive, shear, and torsional strength and elastic modulus. To add specific strength and rigidity to fiber-based composites, Kevlar fibers are incorporated into a variety of topologies, including woven patterns (such as plain, twill, or satin weaves), braided yarn in bi- or tri-dimensional configurations, and unidirectional long or chopped fibers. The composite's matrix component imparts stiffness and stability (Praveenkumara et al., 2022).

The fundamental flaw of the epoxy matrix, which limits its usage, is lower tensile strength, which is caused by excessive cross-linking concentration and the stress distribution created during curing. Numerous secondary nanofillers have augmented it to address the problem of poor yield stress, including nanosilica, carbon nanofibers, graphene, fumed silica, and rubber nanoparticles (Hemanth et al., 2017; Mannan et al., 2022). Epoxy nanocomposite is a secondary phase strengthened by nanofillers. The term “fiber-reinforced epoxy nanocomposite” refers to an epoxy nanocomposite that contains fiber as a reinforcement. Selecting the proper nanosized additives for sophisticated polymeric composites improves the effectiveness of organic composites (Chowdhury et al., 2021; Jawaid et al., 2022). As a result, adding nanofiller to existing fillers creates cutting-edge composites with numerous benefits. A much larger surface region between fillers and the polymer matrices is created per unit of volume due to the increased incidence angle of nanosized additives (Nayak et al., 2022). Consequently, this type of nanocomposite has excellent versatility, high strength, stiffness, lightweight, and corrosion-resistant qualities. The addition of nanofiller has improved tensile, thermostability, electromagnetic, and anaerobic decomposition qualities (Ramesh et al., 2022). Regarding metallic and metal oxide nanomaterials as reinforcement agents in fiber-reinforced composites, TiO<sub>2</sub> nanoparticles are thought to be the most popular nanofiller now available. Amazing specificity, excellent dispersion, high adhesion, superior thermal resilience, and strong chemical cleanliness are some of titanium oxide's appealing characteristics (Alsaadi et al., 2017; Maharana et al., 2021). However, the expense of such nanoparticles is by far their biggest drawback, although this is offset by employing a modest quantity of nanofiller. Optimum mechanical qualities are often only possible with minimal filler loading (Santhosh et al., 2018).

TABLE 1 typical properties of reinforcement and fillers.

| Sl. no. | Material property                                | Value         |
|---------|--|---------------|
| 1       | Density of Kevlar (g/cm <sup>3</sup> )           | 1.53          |
| 2       | % of elongation of Kevlar                        | 3.29          |
| 3       | gsm of the Kevlar mat (g/m <sup>2</sup> )        | 200           |
| 4       | Young's modulus of Kevlar (GPa)                  | 73            |
| 5       | Diameter of the Kevlar filament (cm)             | 0.0014–0.0015 |
| 6       | TiO <sub>2</sub> particle purity                 | 99.12%        |
| 7       | TiO <sub>2</sub> particle size                   | 30 nm         |
| 8       | Density of TiO <sub>2</sub> (g/cm <sup>3</sup> ) | 4.21          |
| 9       | Boiling point of TiO <sub>2</sub> (°C)           | 2,991         |

**TABLE 2** Materials and their levels for nanocomposite.

| Sl. no. | Constraint                  | Symbol | Minimum | Maximum |
|---------|-----------------------------|--------|---------|---------|
| 1       | Kevlar fiber type (gsm)     | A      | 100     | 200     |
| 2       | Nano-TiO <sub>2</sub> (wt%) | B      | 2       | 6       |
| 3       | Cryogenic treatment (min)   | C      | 10      | 30      |

**TABLE 3** ANOVA analysis of tensile behavior.

| Source                              | SOS      | df | MS     | F-value | p-value |
|-------------------------------------|----------|----|--------|---------|---------|
| Model                               | 1,479.15 | 9  | 164.35 | 49.71   | <0.0001 |
| A: Kevlar mat type                  | 44.76    | 1  | 44.76  | 13.54   | 0.0079  |
| B: Weight ratio of TiO <sub>2</sub> | 292.42   | 1  | 292.42 | 88.45   | <0.0001 |
| C: Cryogenic treatment              | 157.62   | 1  | 157.62 | 47.68   | 0.0002  |
| AB                                  | 75.89    | 1  | 75.89  | 22.96   | 0.002   |
| AC                                  | 585.16   | 1  | 585.16 | 177     | <0.0001 |
| BC                                  | 276.72   | 1  | 276.72 | 83.7    | <0.0001 |
| A <sup>2</sup>                      | 36.38    | 1  | 36.38  | 11      | 0.0128  |
| B <sup>2</sup>                      | 5.49     | 1  | 5.49   | 1.66    | 0.2385  |
| C <sup>2</sup>                      | 4.93     | 1  | 4.93   | 1.49    | 0.2614  |
| Residual                            | 23.14    | 7  | 3.31   |         |         |
| Lack of fit                         | 1.78     | 3  | 0.5938 | 0.1112  | 0.9491  |
| Pure error                          | 21.36    | 4  | 5.34   |         |         |
| Cor. total                          | 1,502.29 | 16 |        |         |         |

**TABLE 4** ANOVA analysis of bending behavior.

| Source                              | SOS      | df | MS     | F-value | p-value |
|-------------------------------------|----------|----|--------|---------|---------|
| Model                               | 1,487.23 | 9  | 165.25 | 46.74   | <0.0001 |
| A: Kevlar mat type                  | 35.62    | 1  | 35.62  | 10.07   | 0.0156  |
| B: Weight ratio of TiO <sub>2</sub> | 317.65   | 1  | 317.65 | 89.85   | <0.0001 |
| C: Cryogenic treatment              | 157.62   | 1  | 157.62 | 44.58   | 0.0003  |
| AB                                  | 59.14    | 1  | 59.14  | 16.73   | 0.0046  |
| AC                                  | 585.16   | 1  | 585.16 | 165.52  | <0.0001 |
| BC                                  | 276.72   | 1  | 276.72 | 78.27   | <0.0001 |
| A <sup>2</sup>                      | 40.3     | 1  | 40.3   | 11.4    | 0.0118  |
| B <sup>2</sup>                      | 7.07     | 1  | 7.07   | 2       | 0.2001  |
| C <sup>2</sup>                      | 8.72     | 1  | 8.72   | 2.47    | 0.1604  |
| Residual                            | 24.75    | 7  | 3.54   |         |         |
| Lack of fit                         | 2.14     | 3  | 0.7142 | 0.1264  | 0.9396  |
| Pure error                          | 22.61    | 4  | 5.65   |         |         |
| Cor. total                          | 1,511.98 | 16 |        |         |         |

The hybridization of lightweight materials with more than one reinforcement component, such as fibrous materials, has been extensively studied. Investigators have attached great importance to hybrid reinforced composites because of their special ability to customize mechanical properties (Friedrich, 2018). Fiberglass, carbon, Kevlar, and basalt are frequently used as reinforcing materials in hybrid composites and a few nanoscale nanoparticles. Since it has the greatest mechanical properties and dimensional stability of any reinforcement, Kevlar fiber is one of the most commonly used hybrids in natural fiber composites (Matykiewicz, 2020; Hussian Siyal et al., 2021). Due to its high cost and lack of recyclability, this fiber is regarded as ineffective, despite its excellent strength and rigidity. There are several important benefits to adding titanium dioxide (TiO<sub>2</sub>) filler to Kevlar composite materials. It improves the material’s mechanical qualities, such as impact resistance and tensile strength, making it more resilient and appropriate for structural uses. TiO<sub>2</sub> offers superior UV protection for outdoor and aerospace applications, reducing material deterioration from prolonged sun exposure. Additionally, it lessens water absorption and increases thermal stability, which is critical for applications requiring moisture and heat resistance. Additionally, TiO<sub>2</sub> can affect electrical and dielectric characteristics for applications such as electronics, and it enhances

flame resistance, making it important in fire safety applications. Overall, Kevlar composites perform better, are more durable, and are more appropriate for various applications when TiO<sub>2</sub> filler is added. The increasing use of Kevlar materials in cryogenic environments is a new field. Artificial materials composed of fibers can have better mechanical qualities owing to their cold features (Yogesh et al., 2022; Velmurugan and Natrayan, 2023). For example, materials used to build airplanes should be able to withstand extreme heat or cooling rates of up to 200 °C (Xu et al., 2017; Kara et al., 2018). Cryogenically processed lightweight materials and their matrix have greater strength, are often more durable, and have better durability and abrasion resistance. Consequently, liquid N<sub>2</sub> processing of materials may become a crucial feature of innovative products to enhance the characteristics of composites made from organic resources (Zhang et al., 2009; Sethi et al., 2015).

Investigating how well these hybrid materials work in a cryogenic setting is novel. Due to thermal expansion and embrittlement, freezing temperatures can substantially affect the mechanical properties of a substance. An exciting research component examines how hybrid materials maintain or improve their mechanical features under difficult circumstances. The current project is unique as it is one of the first to analyze nanocomposite

TABLE 5 ANOVA analysis of impact behavior.

| Source                              | SOS      | df | MS     | F-value | p-value |
|-------------------------------------|----------|----|--------|---------|---------|
| Model                               | 1,502.13 | 9  | 166.9  | 50.93   | <0.0001 |
| A: Kevlar mat type                  | 42.55    | 1  | 42.55  | 12.98   | 0.0087  |
| B: Weight ratio of TiO <sub>2</sub> | 349.01   | 1  | 349.01 | 106.5   | <0.0001 |
| C: Cryogenic treatment              | 157.62   | 1  | 157.62 | 48.1    | 0.0002  |
| AB                                  | 41.93    | 1  | 41.93  | 12.79   | 0.009   |
| AC                                  | 585.16   | 1  | 585.16 | 178.56  | <0.0001 |
| BC                                  | 276.72   | 1  | 276.72 | 84.44   | <0.0001 |
| A <sup>2</sup>                      | 37.86    | 1  | 37.86  | 11.55   | 0.0115  |
| B <sup>2</sup>                      | 6.07     | 1  | 6.07   | 1.85    | 0.2156  |
| C <sup>2</sup>                      | 5.49     | 1  | 5.49   | 1.67    | 0.2368  |
| Residual                            | 22.94    | 7  | 3.28   |         |         |
| Lack of fit                         | 1.58     | 3  | 0.5265 | 0.0986  | 0.9567  |
| Pure error                          | 21.36    | 4  | 5.34   |         |         |
| Cor. total                          | 1,525.07 | 16 |        |         |         |

with interlaced Kevlar as reinforcement, and nano-TiO<sub>2</sub> as filler in the epoxy matrix in cryogenic temperatures. The findings of this study might pave the way for novel applications of natural fiber-based composite in severe cold conditions.

The fundamental goal of the current research is to build, evaluate, and improve the material features of hybrid composite materials using the following conditions: weight proportions of nano-TiO<sub>2</sub>, thickness of Kevlar fiber in gsm, and duration of cryogenic processing. To complete these objectives, the composites were fabricated hybrid nanocomposites which had been compression-molded. The nanocomposites were fabricated using the following parameters: weight ratio of TiO<sub>2</sub> filler, type of Kevlar mat, and cryogenic treatment duration. After fabrication, the composites were tested, and their impact on process parameters was optimized using RSM and ANN networks. This study offers a

unique combination of materials, investigates how they behave in a difficult setting, employs cutting-edge statistical and machine learning approaches for optimization, and discusses the significance of the results for real-world applications. These add to the topic’s originality.

## 2 Experimental

### 2.1 Materials

Huntsman epoxy resin (AW 106) with a 1.52 g/cm<sup>3</sup> density and hardener HV 953 U were used as matrix materials in the current research. The resin and matrix were procured from Deesh Chemical Industries, Chennai, Tamil Nadu, India. The Kevlar fiber mat (K-129 type with 200 gsm) used as the current study’s reinforcement was purchased from Rithu Recourses, Salam, India. The filaments were splashed in clean water before use and dehydrated in an oven at 75 °C. The highest purity and quality titanium oxide (TiO<sub>2</sub>) was purchased from Naga Chemical Industry in Chennai, Tamil Nadu, India. Table 1 shows some typical properties of the reinforcement and fillers.

For composite preparations, 200 gsm (grams per square meter) of Kevlar fiber was preferred since it improves mechanical qualities and structural integrity and meets application-specific criteria. Improved strength, better load-bearing ability, and improved durability against delamination are all made possible by Kevlar fiber’s higher gsm, resulting in a composite product with superior hardness and impact resistance. In order to ensure that the composite satisfied the required performance objectives and was well-suited for its intended use—whether in aviation, the military, automobiles, or other sectors—the decision was frequently dictated by the particular demands of the application.

### 2.2 Fabrication of hybrid composites

The composite was fabricated using compression molding. In the first step, we mixed the different weight proportions of nano-

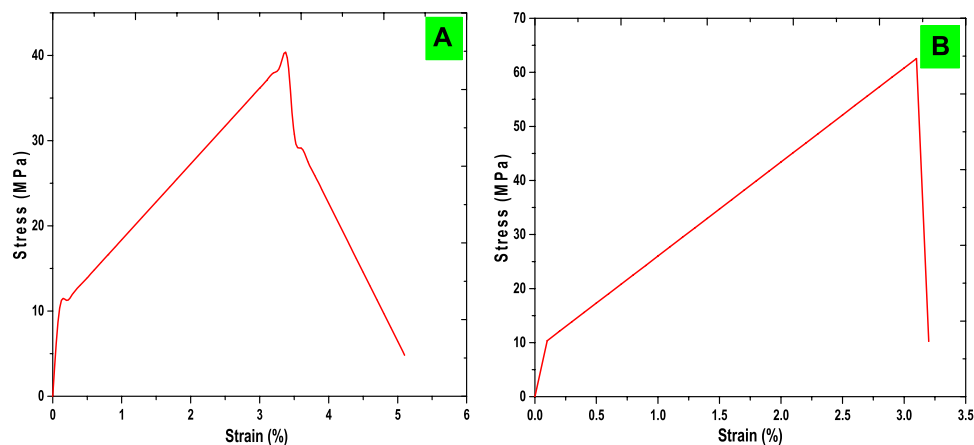
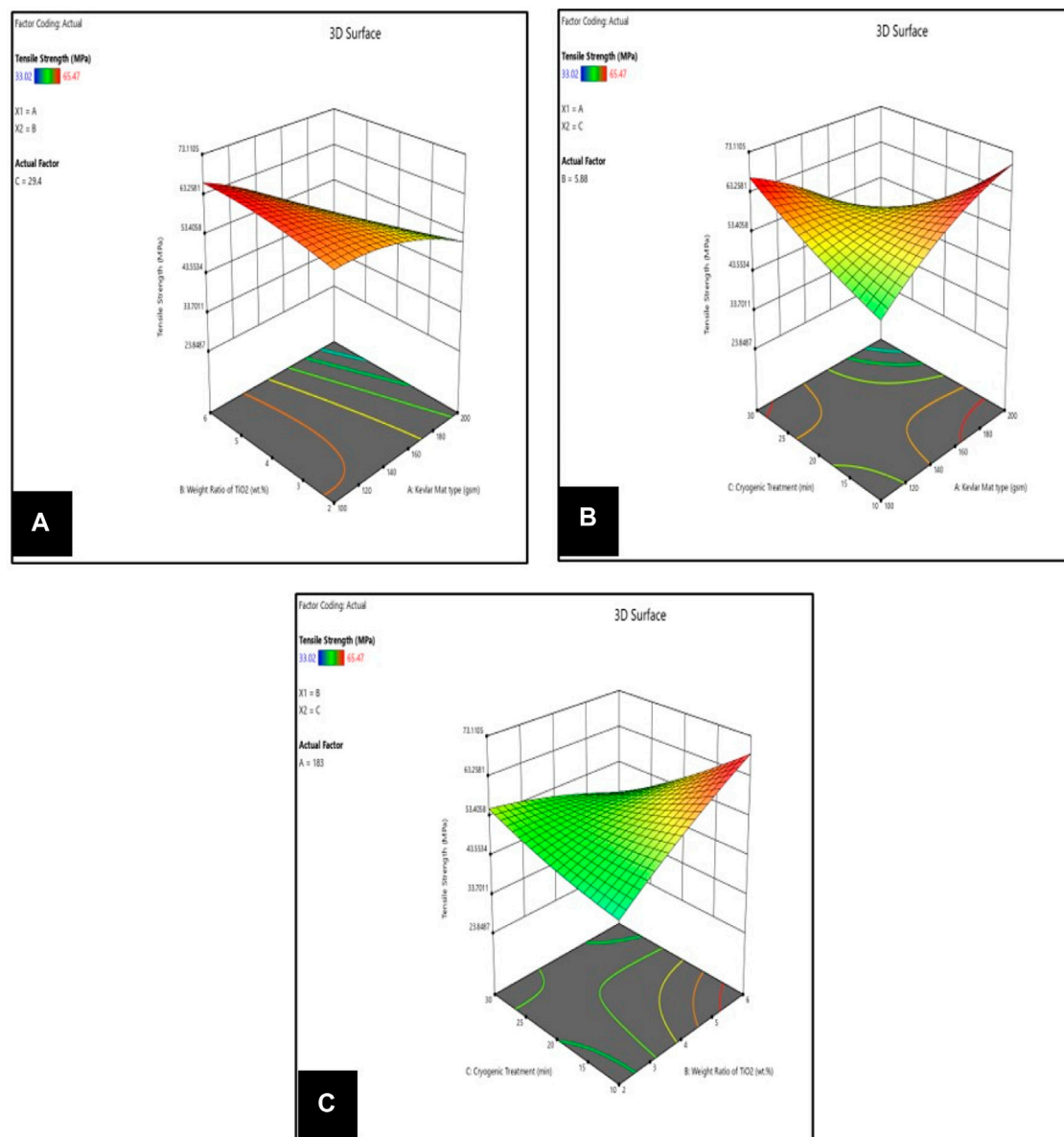


FIGURE 1 Stress-strain relationship of (A) tensile strength; (B) flexural strength.



**FIGURE 2** Tensile behavior of TiO<sub>2</sub>/Kevlar-based nanocomposites, (A) Kevlar Mat type vs. Weight ratio of TiO<sub>2</sub> vs. Tensile strength; (B) Kevlar Mat type vs. Cryogenic treatment vs. Tensile strength; (C) Weight ratio of TiO<sub>2</sub> vs. Cryogenic treatment vs. Tensile strength.

TiO<sub>2</sub> particles (2, 4, and 6 wt%) with epoxy resin through an ultrasonicator. This process took approximately 10 min, using ultrasonic waves to help mix them evenly. After mixing, TiO<sub>2</sub> and epoxy were mixed in a special tube, and high-frequency sound waves were used to further mix them for 30 min. After that, the hardener was added to an epoxy–nanofiller mixer in a suitable weight proportion (10:1). Then the prepared mixer was poured into the Kevlar fiber mat, which was placed into a 300 × 300 × 3 mm metallic mold. Finally, the prepared mold was placed into the compression molding machine. The temperature and pressure of the compression molding process were maintained at approximately 170 °C and 15 bar, respectively. The same process was repeated up to 17 times to produce 17 different composite plates. Once the compression molding process was completed, the

fabricated hybrid laminates were placed under ambient conditions for 24 h. Finally, the fabricated laminates were cut into different sizes (based on the ASTM standard) to examine their mechanical properties. Table 2 displays the composite’s features and respective concentrations.

### 2.3 Cryogenic treatment

A regulated high-temperature liquid chamber with preprogrammed controllers was utilized for the cryogenic rehabilitation process. The temperature was cooled to 196 °C using a measured preservation rate (3 °C/min). According to the concept designs, the created samples were submerged in N<sub>2</sub> fluid at



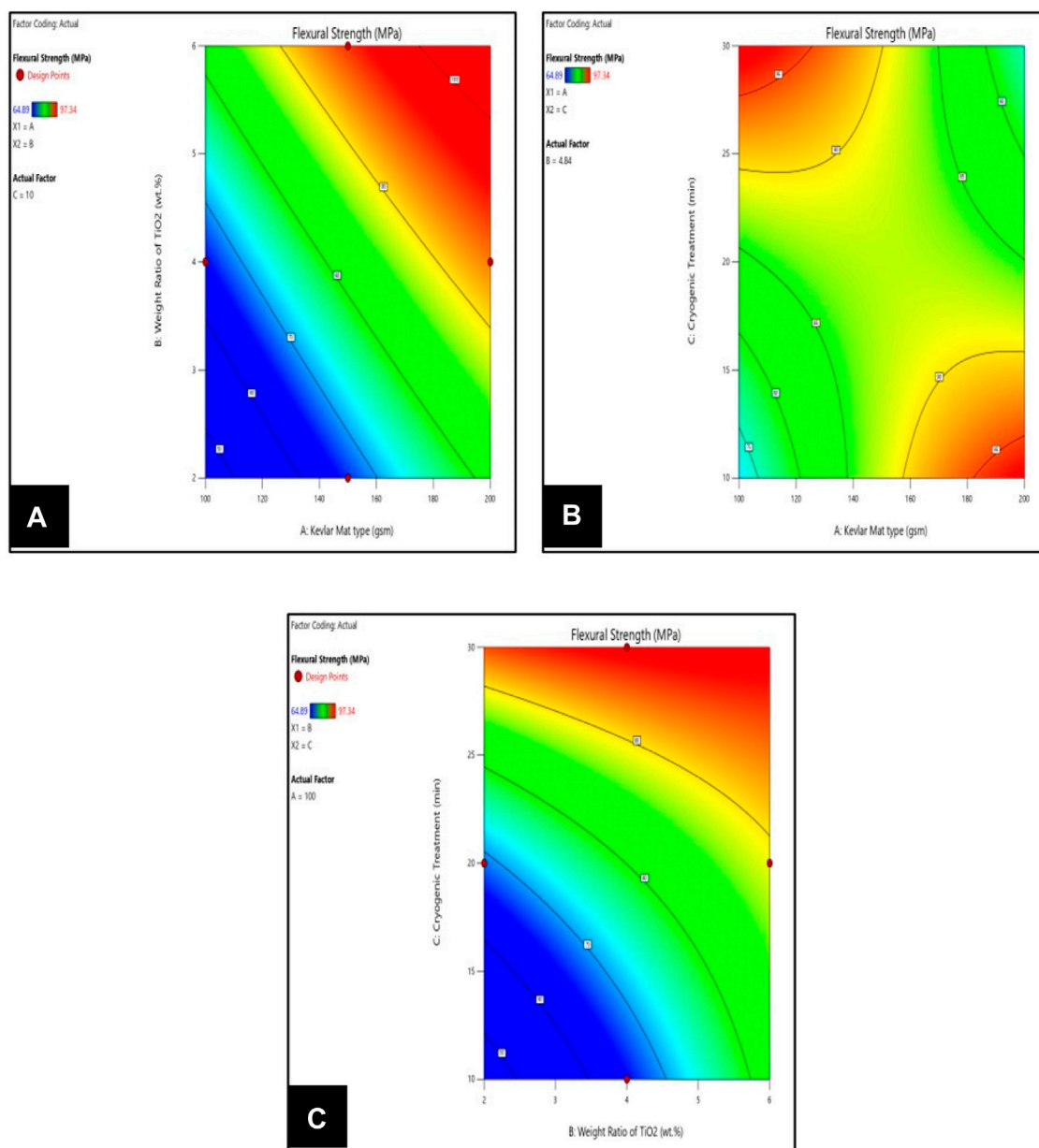


**FIGURE 3** Bending behavior of TiO<sub>2</sub>/Kevlar-based nanocomposites, (A) Kevlar Mat type vs. Weight ratio of TiO<sub>2</sub> vs. Flexural strength; (B) Kevlar Mat type vs. Cryogenic treatment vs. Flexural strength; (C) Weight ratio of TiO<sub>2</sub> vs. Cryogenic treatment vs. Flexural strength.

77 K for 10, 20, and 30 min of cold working. After preparation, the composite was periodically warmed to an ambient temperature of 40°C/h.

### 2.4 Response surface methodology

Response surface methodology (RSM) is a combination of quantitative methodologies that can be utilized to examine data and their interaction effects through analytical trials to simultaneously build and resolve multidimensional problems. RSM is a geometrically based method used to estimate and

describe the experimentally ideal conditions and a polynomial equation to construct a relationship between direct and indirect parts. A well-known RSM concept for enhancing strength properties is the Box–Behnken design (BBD). All longitudinal, nonlinear, and two different relationships were estimated using the spinning lesser designs that constitute the Box–Behnken model. Design decrease is not permitted; there are no corners in the design process. The axis endpoints are outside the rotating full factorial entity’s created visual studio container. The direction from the center of the design enabled the anticipated response to be calculated with the same variation. As shown in Table 1, extraction experiments utilizing BBD were conducted on three factors: Kevlar fiber mat (A), weight ratio of

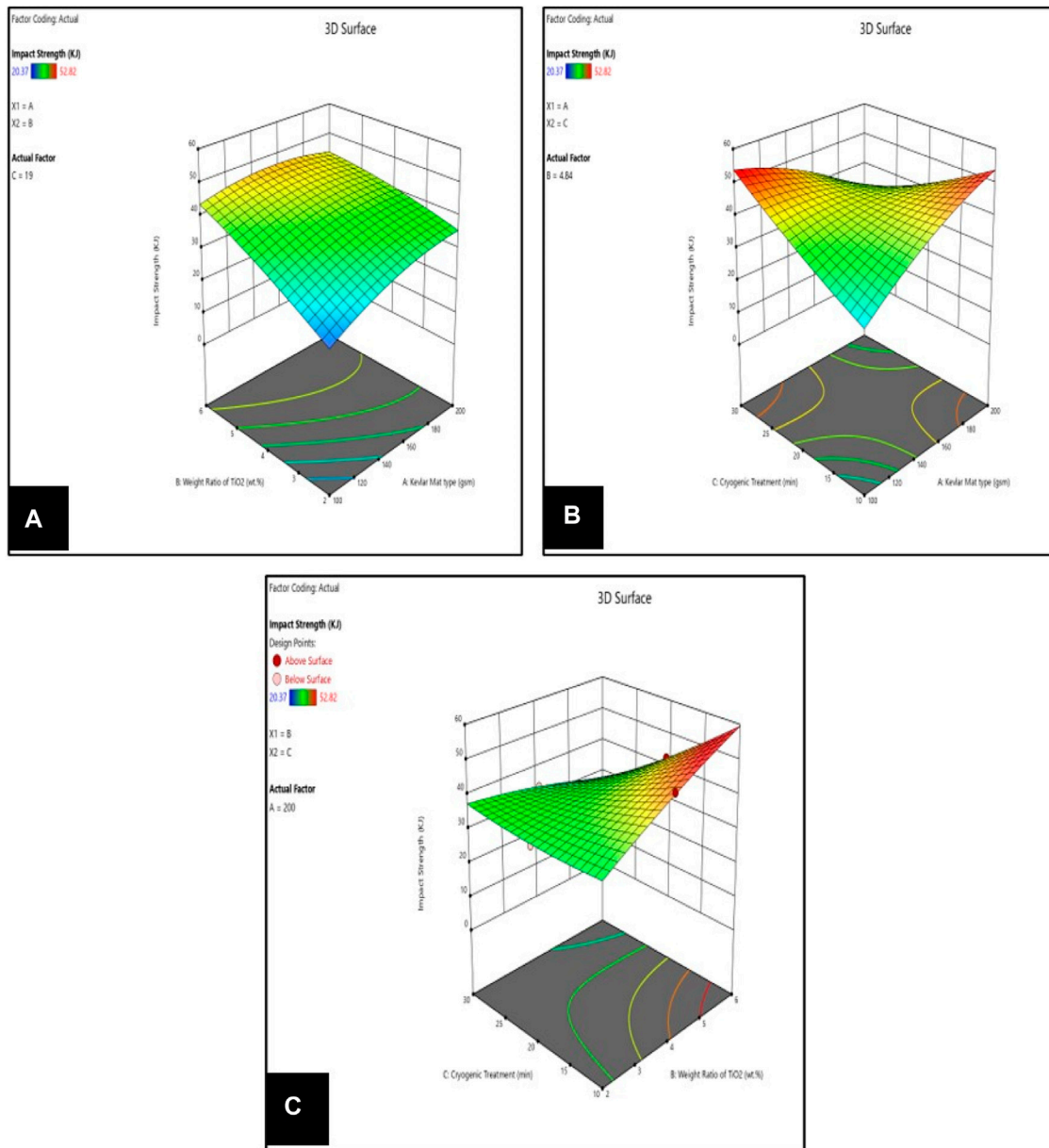


**FIGURE 4** Impact behavior of TiO<sub>2</sub>/Kevlar-based nanocomposites, **(A)** Kevlar Mat type vs. Weight ratio of TiO<sub>2</sub> vs. Impact strength; **(B)** Kevlar Mat type vs. Cryogenic treatment vs. Impact strength; **(C)** Weight ratio of TiO<sub>2</sub> vs. Cryogenic treatment vs. Impact strength.

Kevlar (B), and cryogenic treatment durations (C). Results were calculated using a least-squares method for multi-regression evaluation (Sethi et al., 2015).

$$i = \frac{y_i - y_0}{\Delta y}, \text{ where } i = 1, 2, 3, \tag{1}$$

where *i* stands for a coding number of a self-determining component, *y<sub>i</sub>* for its actual value, *y<sub>0</sub>* for its real value depending on the middle, and *y* for its modifying requirements. In the BBD, a cluster of spots only exists at the halfway point of an edge piece and the simulated center of the multidimensional blocks. The average results from a set of process conditions were utilized after three test iterations. The quadratic polynomial equation may be employed to prompt the

quantitative response surface on such variables in a configuration with the three primary self-determining elements, Y1, Y2, and Y3 (2):

$$X = \partial_0 + \partial_1 Z_1 + \partial_2 Z_2 + \partial_3 Z_3 + \partial_{11} Z_1^2 + \partial_{22} Z_2^2 + \partial_{33} Z_3^2 + \partial_{12} Z_1 Z_2 + \partial_{13} Z_1 Z_3 + \partial_{23} Z_2 Z_3 + \epsilon, \tag{2}$$

where *X* is the expected response, *α<sub>0</sub>* is the perfect quantities, *Z<sub>1</sub>*, *Z<sub>2</sub>*, and *Z<sub>3</sub>* are momentous influences, *∂<sub>1</sub>*, *∂<sub>2</sub>*, and *∂<sub>3</sub>* are rectilinear factors; *∂<sub>12</sub>*, *∂<sub>13</sub>*, and *∂<sub>23</sub>* are creation irritated command factors; *∂<sub>11</sub>*, *∂<sub>22</sub>*, and *∂<sub>33</sub>* are quadratic polynomial factors. The quadratic model calculation’s fitting level was described using the *R*<sup>2</sup> correlation ratio. The melting of the polyolefin used in this study controlled the variables, including pressure, duration, and

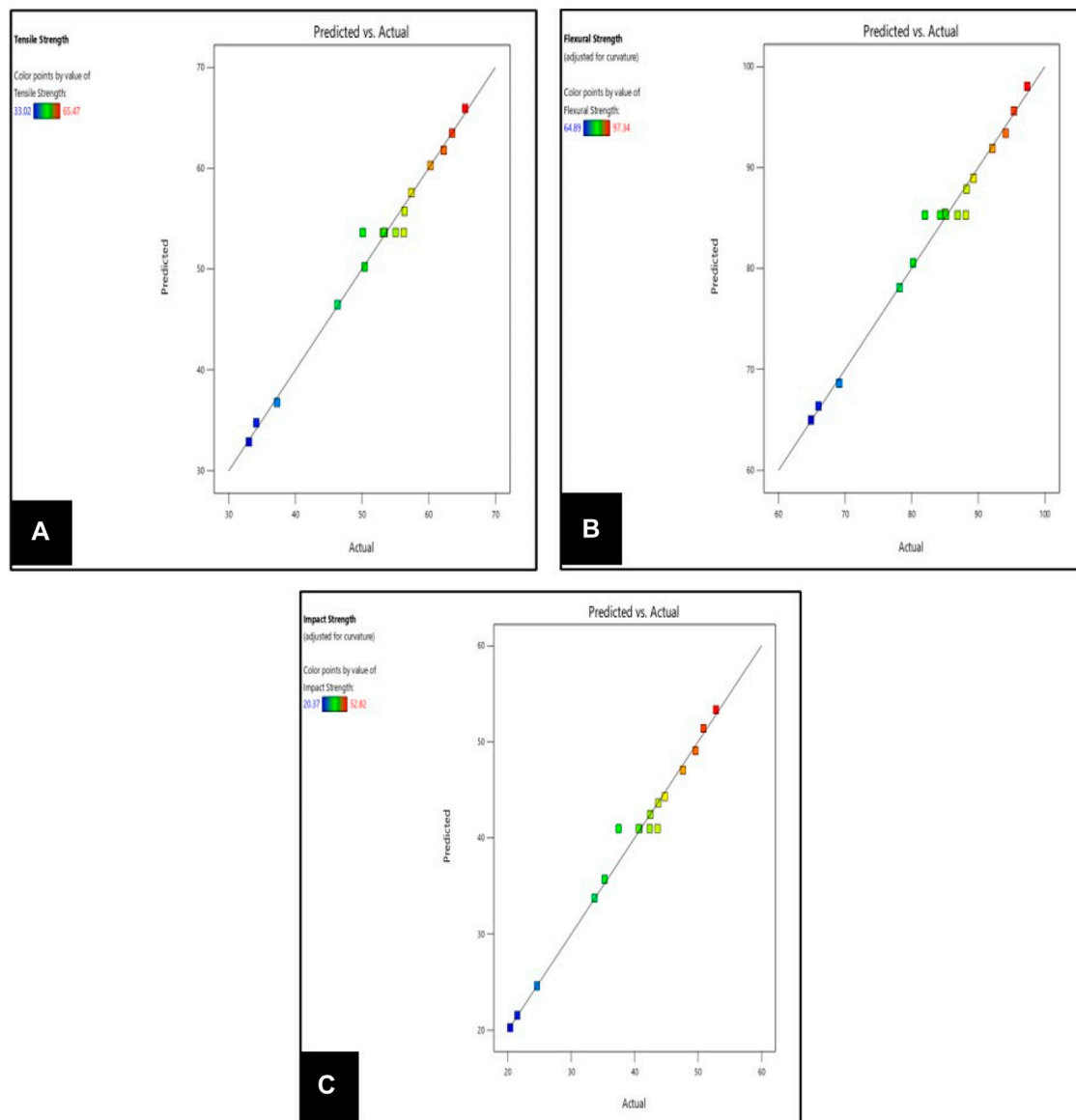


**FIGURE 5** Actual vs. predicted values of TiO<sub>2</sub>/Kevlar-based hybrid nanocomposites, (A) tensile; (B) flexural; and (C) impact behaviors.

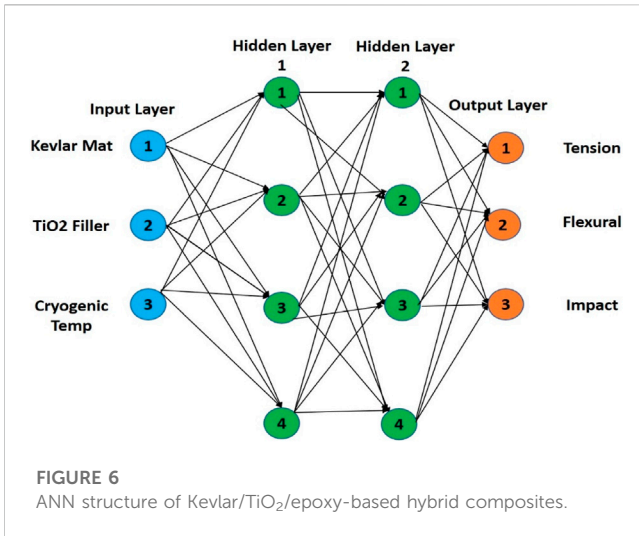
temperature. Manifold rectilinear deterioration investigation yielded the factors, and the computation could be employed to regulate the consequences. For such an inquiry, BBD with three aspects was chosen as the level of testing (Hemanth et al., 2017; Velmurugan et al., 2023).

### 2.5 Composite sample testing

The tensile characteristics of both primary and hybridized materials were tested according to the ASTM D3039-76 standard. The sample measured 250 × 25 × 3 mm. According to the ASTM D3039-76 regulation, the gauge length throughout the experiment was 150 mm, and the crosshead speeds were 2 mm/min. Measurements were made of the tensile

characteristics, strain, and modulus of dry and saltwater-aged materials. The test was conducted using Instron-3389 Universal Testing Equipment. Three specimens of each type were used to examine them, and the average information was then published. This bending test was carried out according to ASTM D7264 specifications. The sample measured 70 × 12.7 × 3. The depth ratio for most of the experiment’s span length of 60 mm was 20:1. Utilizing the ASTM D256 criteria, the impact strength of both the original and hybridized composites was assessed. A 65 × 12.7 × 3 mm specimen was employed for the evaluation. Every specimen was examined three times, with the average result being noted. The fracture surface of the fabricated composites was examined through a scanning electron microscope (SEM). This mechanical and morphological analysis was conducted at SRM University, Chennai, Tamil Nadu, India.





### 3 Results and discussion

#### 3.1 Response surface models

The RSM method for the mechanical features of hybridized fiber composites of Kevlar and nano-TiO<sub>2</sub> is as follows: this study discovered that the tension, bending, and shock resistance values of the connection factor (*R*<sup>2</sup>) were, respectively, 0.9846, 0.9836, and 0.9850, proving the method’s suitability and the generated parameter’s precision. It is obvious that the relationships between tensile properties and respective components effectively compensate for information errancy. In Eqs 3–5, the symbols A, B, and C represent the Kevlar fiber types, TiO<sub>2</sub> filler weight proportions, and cryogenic treatment durations, respectively.

$$\text{Tensile Strength} = 53.62 + 2.37A + 6.05B + 4.44C - 4.36AB - 12.10AC - 8.32BC - 2.94A^2 - 1.14B^2 + 1.08C^2, \quad (3)$$

$$\text{Flexural Strength} = 85.29 + 2.11A + 6.30B + 4.44C - 3.85AB - 12.10AC - 8.32BC - 3.09A^2 - 1.30B^2 - 1.44C^2, \quad (4)$$

$$\text{Impact Strength} = 40.97 + 2.31A + 6.61B + 4.44C - 3.24AB - 12.10AC - 8.32BC - 3A^2 - 1.20B^2 + 1.14C^2. \quad (5)$$

#### 3.1.1 Analysis of developed mathematical models

The ANOVA approach often controls the RSM design and its variables’ adequacy and relevancy. The F-value is used to determine the suitability of the model. The ANOVA outcomes for the material characteristics of mixed lightweight materials are displayed in Tables 3–5. Using a prototypical F-value of 49.47, Table 3 demonstrates that the cubic model is adequate for forecasting ductility. Table 2 shows that the F rate of a quadratic equation prototype is below 0.0001, demonstrating that the prototypical is substantial. Furthermore, this study explores the diverse impacts of different Kevlar fiber types (labeled as A) and nano-TiO<sub>2</sub> (designated as B) on crucial models (Sabarinathan et al., 2022).

Using a prototypical F rate of 46.74, Table 4 demonstrates that the cubic prototypical is suitable for forecasting bending behavior. The “Prob > F” rate of a quadratic equation prototypical is below 0.0001, indicating that the prototypical is substantial. Similarly, the impact behavior results were achieved with an F-value of 50.93. The weight ratio of the nano-TiO<sub>2</sub> models in the Kevlar fiber type (A) and (B) models is also important. In addition to the previously listed models, some others are less evident. Moreover, the weight proportion of the nano-TiO<sub>2</sub> models in Kevlar fiber type (A) is important. A couple more are not immediately apparent in addition to previously described models. Figure 1 shows the stress–strain relationship of tensile and flexural behavior.

The influence of fiber thickness (gsm) on the mechanical behaviors of Kevlar–nano-TiO<sub>2</sub>-mixed epoxy composite, such as

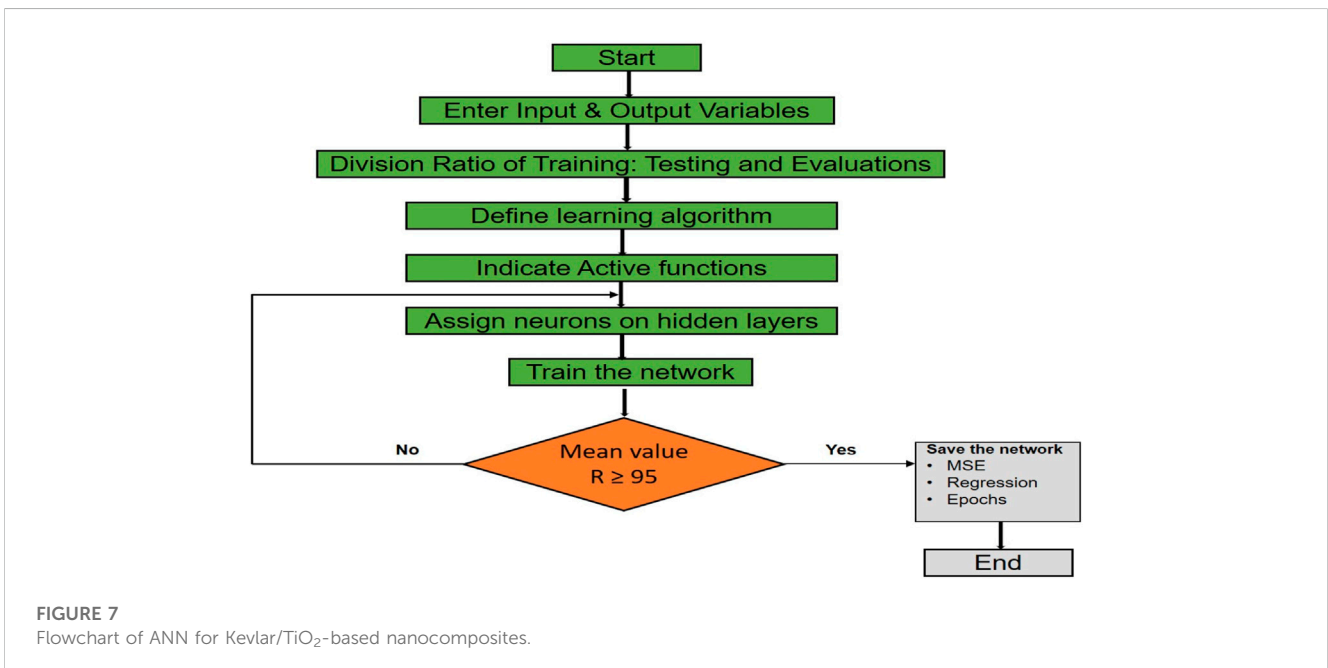


TABLE 6 Comparison of experimental/ANN/error of a nanocomposite.

| Run | Experimental result |          |        | ANN result |          |        | Predicted error |          |        |
|-----|---------------------|----------|--------|------------|----------|--------|-----------------|----------|--------|
|     | Tensile             | Flexural | Impact | Tensile    | Flexural | Impact | Tensile         | Flexural | Impact |
| 1   | 65.47               | 97.34    | 52.82  | 66.12      | 97.89    | 53.05  | -0.993          | -0.565   | -0.435 |
| 2   | 34.13               | 66       | 21.48  | 34.35      | 66.05    | 21.48  | -0.645          | -0.076   | 0.000  |
| 3   | 37.25               | 69.12    | 24.6   | 37.47      | 69.15    | 24.6   | -0.591          | -0.043   | 0.000  |
| 4   | 57.41               | 89.28    | 44.76  | 57.63      | 89.35    | 44.76  | -0.383          | -0.078   | 0.000  |
| 5   | 56.36               | 88.23    | 43.71  | 56.58      | 88.34    | 43.71  | -0.390          | -0.120   | 0.000  |
| 6   | 50.12               | 81.99    | 37.47  | 50.34      | 82.10    | 40.54  | -0.439          | -0.129   | -8.193 |
| 7   | 62.25               | 94.12    | 49.6   | 62.47      | 94.12    | 44.91  | -0.353          | 0.000    | 9.456  |
| 8   | 63.5                | 95.37    | 50.85  | 63.72      | 94.20    | 50.85  | -0.346          | 1.227    | 0.000  |
| 9   | 46.32               | 78.19    | 33.67  | 46.54      | 78.30    | 33.67  | -0.475          | -0.136   | 0.000  |
| 10  | 53.29               | 85.16    | 40.64  | 53.51      | 85.05    | 40.54  | -0.413          | 0.129    | 0.246  |
| 11  | 55.03               | 86.9     | 42.38  | 55.25      | 87.01    | 40.54  | -0.400          | -0.122   | 4.342  |
| 12  | 33.02               | 64.89    | 20.37  | 33.24      | 63.25    | 20.37  | -0.666          | 2.527    | 0.000  |
| 13  | 56.26               | 88.13    | 43.61  | 56.48      | 88.24    | 40.54  | -0.391          | -0.120   | 7.040  |
| 14  | 60.26               | 92.13    | 47.61  | 60.48      | 92.24    | 47.61  | -0.365          | -0.115   | 0.000  |
| 15  | 53.12               | 84.99    | 42.47  | 53.34      | 85.10    | 42.47  | -0.414          | -0.125   | 0.000  |
| 16  | 53.41               | 84.27    | 40.76  | 53.63      | 84.12    | 40.54  | -0.412          | 0.178    | 0.540  |
| 17  | 50.383              | 80.21    | 35.26  | 50.60      | 80.24    | 35.26  | -0.437          | -0.037   | 0.000  |

tension, bending, and impact strength, is depicted in Figures 2A–C. The finest mechanical properties of Kevlar fiber are 200 gsm, which is superior to 100 gsm and 150 gsm. Poor levels at 100 gsm composite are due to inadequate load transmission caused by uneven fiber dispersion throughout matrices. Consequently, the composites industrialized a lattice district through a feeble fiber-to-fiber interface. The composite material was ripped out of the matrix when added in this condition. This illustrates that the 100 gsm contributing positively to the Kevlar fiber composite is inadequate for maintaining the mechanical stress. The composite's mechanical properties improve when the mixture's fiber is raised from 100 gsm to 200 gsm. This is primarily attributable to the fibers and matrix forming a strong link that prevented gaps in the composites by accepting additional fibers and maintaining proper load distribution. The collaboration between the reinforcement and the resin improved the fiber quantity. Consequently, more power is necessary to disrupt the link between the interlaced cellulose fibers (Mannan et al., 2022; Mohit et al., 2023).

The efficacy of the bending characteristics of the nano-TiO<sub>2</sub> filler additives is shown in Figures 3A–C. Four weight percentages (4 wt%) of nano-TiO<sub>2</sub> showed greater mechanical strength than 2 wt% and 6 wt%. A 4 wt% content of nano-TiO<sub>2</sub> in resin may have better stress distribution and transmission, explaining its improved mechanical properties. The number and size of holes in the polymeric matrix improved with the addition of more loaded TiO<sub>2</sub>, which impacted the decohesion binding between the matrix and the reinforcement (Alsaadi et al., 2017; Hussian Siyal et al., 2021). Incorporating much more filled TiO<sub>2</sub> into the polymeric matrix enhanced the permeability and

diameter of the pores, which influenced the decohesion binding between fibers and matrix. Consequently, the adhesion, interwoven Kevlar, and combined nanoscale padding formulations produced adequate adhesives between surface nerve entrapment at a concentration of 4 wt%. Furthermore, the inclusion of 2 wt% and 6 wt% TiO<sub>2</sub> resulted in a poor outcome, showing decreased strength properties. Moreover, 2 wt% and 6 wt% concentrations exhibited poor boundary adhesive of composites in woven Kevlar and polymeric, resulting in agglomerate due to poor adhering and poor hybrid functional capabilities.

During cryogenic treatment, the nanocomposite surface experienced heat fluctuation and was visible in fluid N<sub>2</sub> at -196 °C. Cryo-ablation is an exclusive approach to progressing thermoplastic nanocomposites' material properties. Figures 4A–C shows how polymer-based hybrid composites' mechanical properties are affected by cryogenic handling, which may be caused by the residual pressure formed through the firmness interface due to the compound substance's freezing effort. Residual strains are produced at low temperatures due to the shifting matrices and fiber contraction. This interfacial stress helps maintain a relationship between the reinforcement and resin and improves adhesion, leading to improved results, although this is only feasible for the first 20 min. Thereafter, the composites' mechanical characteristics decreased. This could occur due to layer-specific microcracking, potholing, or excessive stress (Sethi et al., 2015; Ganesan et al., 2020; Velmurugan and Babu, 2020). Figures 5A–C demonstrates the RSM values of actual and predicted values of TiO<sub>2</sub>-based hybrid composites.

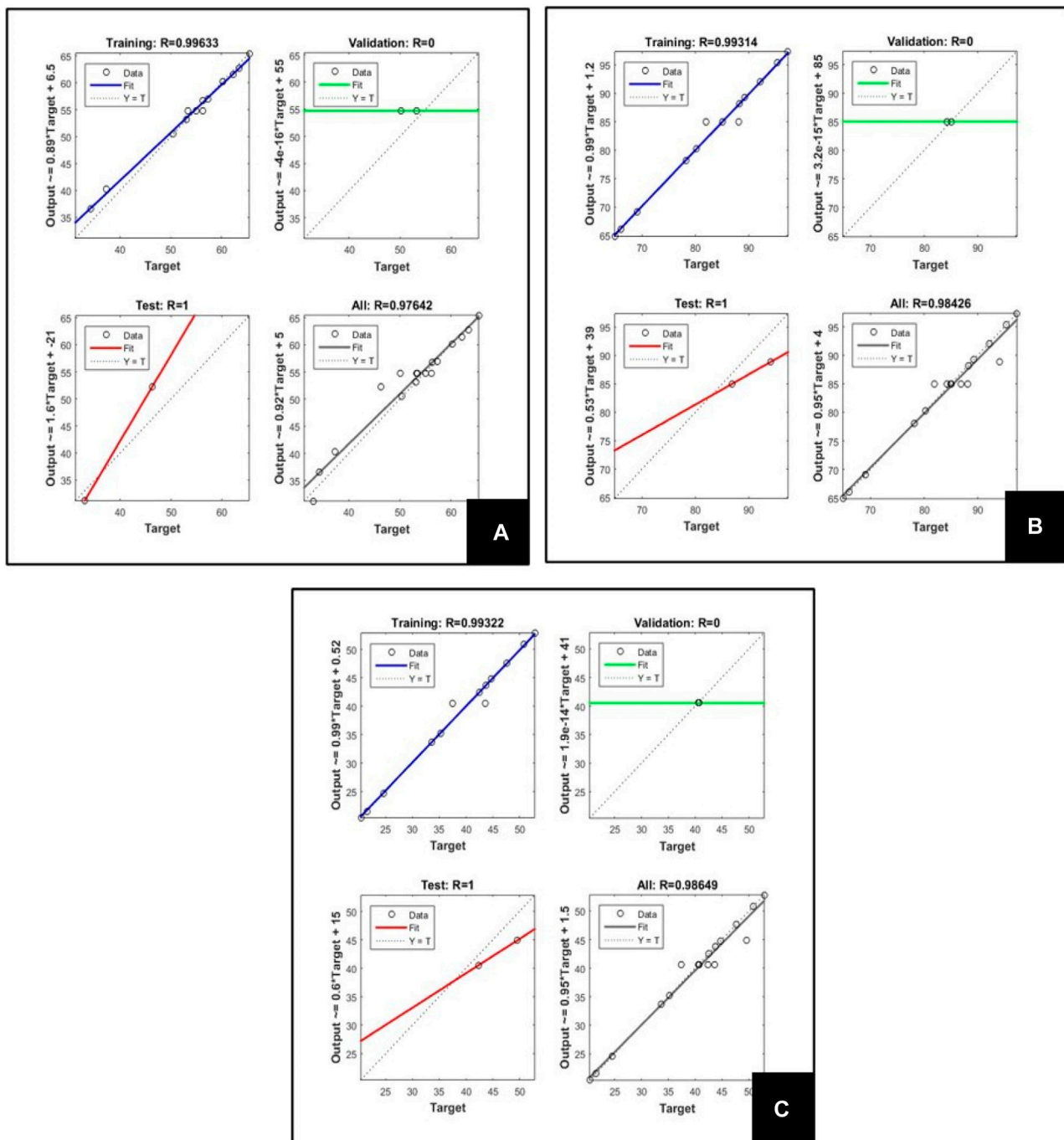


FIGURE 8 Performance features of the ANN model: (A) tensile; (B) flexural; and (C) impact behaviors.

### 3.2 Artificial neural network

It is widely known that modeling and analysis of the extraction procedure may anticipate the extraction method and complex linkages. A useful tool for interpreting the link between inputs and enhanced experiments is artificial neural networks (ANNs). The ANN model can generalize recently acquired knowledge and learn the structure of the iterative mechanism from historical data. The input, hidden, and output neurons of the ANN model are three

separate layers that could be used to estimate the association between the source and destination nodes. Learning (70%), evaluation (15%), and verification (15%) are the three categories into which all the information is arbitrarily split (Ismail et al., 2022; Pragadish et al., 2022).

The output of the ANN model is assessed using the performance indicators of mean square and regression coefficients. The toolkit of MATLAB Version R2015 was used to run the ANN calculations for this investigation. We used a three-layer ANN with a

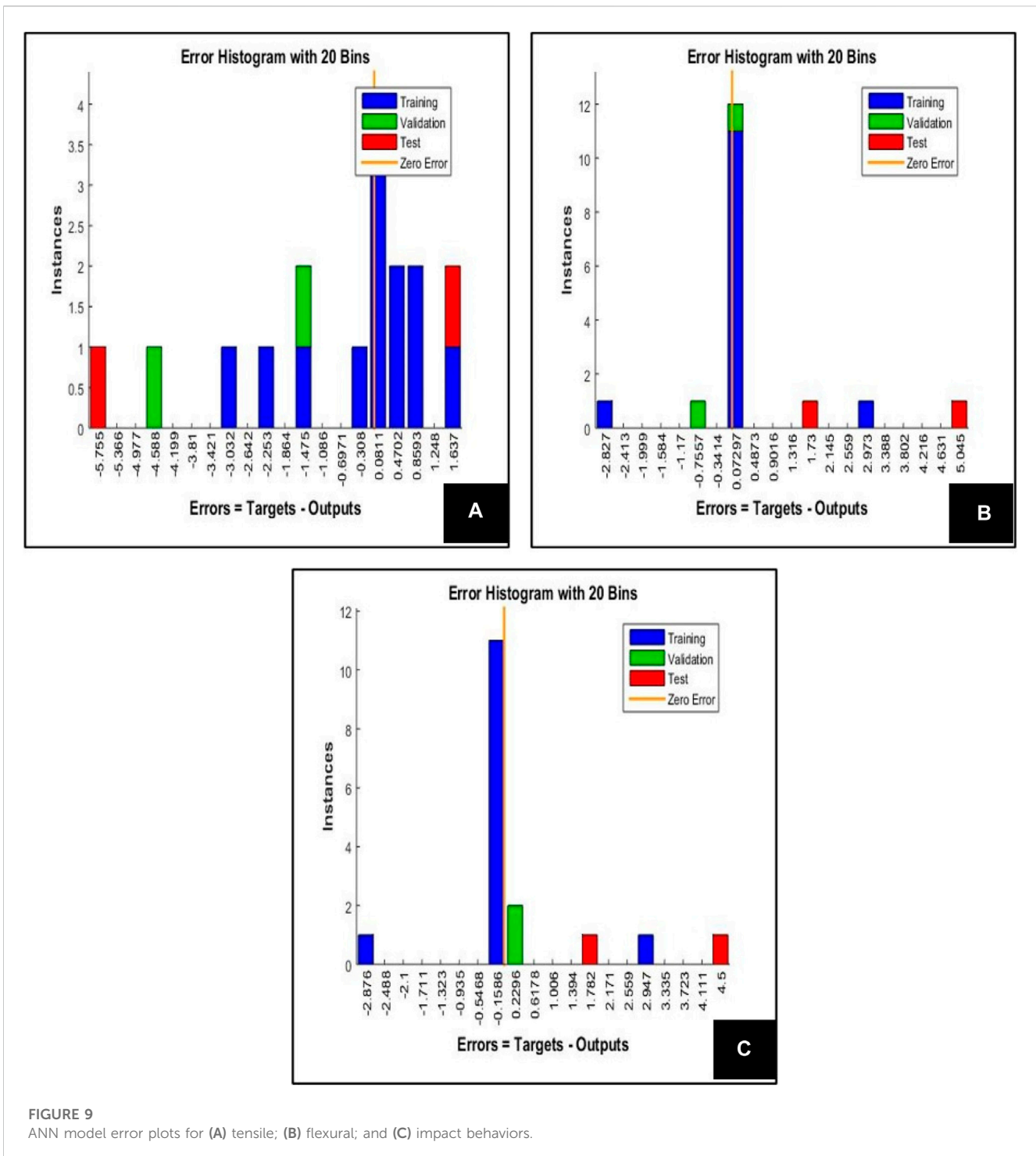
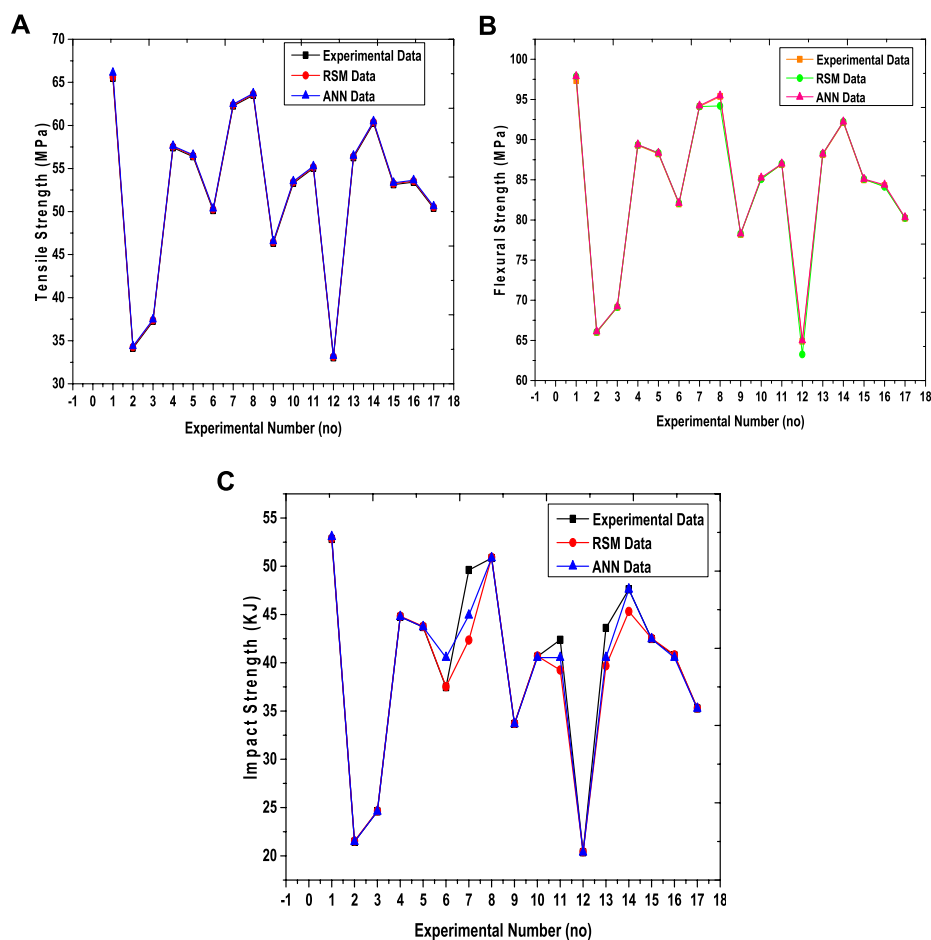


FIGURE 9 ANN model error plots for (A) tensile; (B) flexural; and (C) impact behaviors.

Levenberg–Marquardt back-propagation algorithm of 1,000 steps, a tangential sigmoidal function at the hidden state, and a linear activation functional at the output nodes. After constructing the system, the given statistical models are incorporated into the 4–4–3 ANN design (Figure 6). A correlation matrix and a proportional confidence level were used to evaluate the strategy. The entire flowchart for the ANN predictions is shown in Figure 7. The existing ANN system uses Formula 4 to compute the anticipated average inaccuracy.

$$\% \text{ of Predicted Error} = \frac{\text{Experimental Data} - \text{ANN Data}}{\text{Experimental Data}} \times 100. \tag{6}$$

Table 6 displays the learning, verification, and assessment measurement categories and the estimated error percentage. Figures 8A–C show how well the neurological theory predicts the future. “Tensile” had a reliability of all parameters of 0.9764. The average number of predicted errors fell below 3%, with values of



**FIGURE 10** Comparison of experimental/ANN outcomes of (A) tensile; (B) flexural; and (C) impact behaviors of TiO<sub>2</sub>-based nanocomposites.

**TABLE 7** Optimum outcomes of nanocomposites.

| Outcome        | Parameter      | Investigational | RSM model | ANN model |
|----------------|----------------|-----------------|-----------|-----------|
| Tensile (MPa)  | A3, B2, and C2 | 65.47           | 65.89     | 66.12     |
| Flexural (MPa) | A3, B2, and C2 | 97.34           | 97.52     | 97.89     |
| ILSS (MPa)     | A3, B2, and C2 | 52.82           | 52.96     | 53.05     |

0.9842 for bending and 0.9864 for impact; Figure 9 demonstrates this. Figures 10A–C illustrate the study results and the relationship between network flexibility. Observed variables were within the desired limits, and the investigation was applied to assess the accuracy of experimental data (Hemanth et al., 2017; Santhosh et al., 2018; Devarajan et al., 2021). The reliability of the investigation, prognosis, and ANN models is summarized in Figure 9. The study of experimental data revealed that both the RSM and ANN procedures provide trustworthy outcomes.

Compared to RSM-computed observations, the ANN method produced good outcomes and more reliable forecasts with an accuracy rating of 95%. The ANN optimum model facilitates the integration of the variability contributing to a given cast composition. Since it lowers costs, this is ideal for the parts of

the automotive sector that employ natural fibers. Table 7 displays the mechanical property performance that performs best based on observable, analytical, and ANN results.

### 4 Microstructural analysis

The SEM photographs of Kevlar and Kevlar/TiO<sub>2</sub> hybrid composites are shown in Figures 11A, B. Figure 11A shows the Kevlar fiber strengthened with epoxy. It was discovered that the strands had been pulled out of the polymer and that they developed a crack throughout the fiber. The intricate fiber pattern was a barrier against polymeric distortion and fracture development. Most of the TiO<sub>2</sub> nanoparticles remained well coupled with the polymers for the



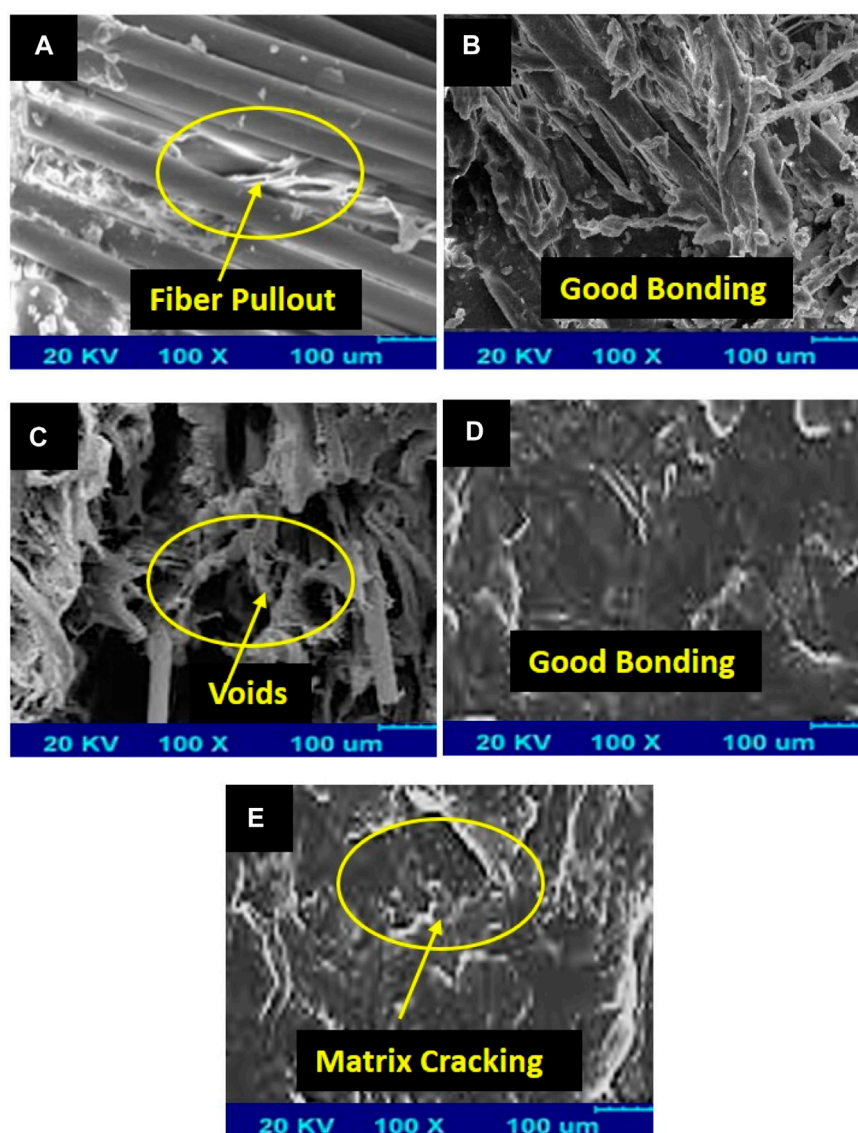


**FIGURE 11**  
Microstructural images of hybrid composites after tensile (MPa) failures of (A) pure Kevlar; (B) Kevlar/4 wt% of TiO<sub>2</sub>; (C) Kevlar/6 wt% of TiO<sub>2</sub>; (D) cryogenic at 20 min treatment, and (E) cryogenic at 30 min treatment.

4 wt% of TiO<sub>2</sub>-reinforced Kevlar fiber epoxy laminated materials, as shown in Figure 11B. This indicates that the TiO<sub>2</sub> nanoparticles were present in the polymer. However, a fracture might form through the pores on the TiO<sub>2</sub> in well-combined TiO<sub>2</sub> nanoparticles, as shown by a thin epoxy polymer film attached to the TiO<sub>2</sub> nanoparticles. The surface of the fracture also appeared to be rough and to include branching, bending cracks, and crack pinning. Spherical silica-reinforced epoxy polymer was also studied for these features (Deka et al., 2005; Yildirim et al., 2021). The outermost layer of fracturing for the 6 wt% TiO<sub>2</sub> and Kevlar fiber-reinforced epoxy polymer was rough, and the spaces surrounding the fillers suggest that the TiO<sub>2</sub> particles may have de-bonded from the polymer. Additionally, Figure 11C shows that fillers tended to collect. TiO<sub>2</sub> nanoparticle buildup served as a carrier of failure that might further weaken the mechanical properties. After 20 and 30 min of cryogenic

treatment, hybrid composites fail, as shown in Figures 11D, E. TiO<sub>2</sub> filler is well bonded to fiber and matrix in Figure 11D. This may have occurred due to compressive stress in the laminate's topmost layer. The matrix's fracture propagation is shown in Figure 11E, which may be due to excessive tension building up in the composite.

## 5 Conclusion

An important development in composite substances and their efficacy in harsh environments may be seen in statistical optimization research employing RSM and ANN approaches. This discovery has revealed new ways of combining Kevlar fibers, epoxy matrix, and TiO<sub>2</sub> filler to obtain improved mechanical qualities, which exceed what these materials are capable of on their own.



- Under this investigation, the lightweight material's performance of TiO<sub>2</sub>-based interlaced Kevlar/epoxy-based hybridization was created and improved using RSM. The process parameter factors for TiO<sub>2</sub>- and Kevlar-influenced lightweight materials were set at 4% TiO<sub>2</sub>, 200 gsm of Kevlar, and 20 min durations of cryogenic processing following the multi-response surface approach. Correspondingly, the correlation coefficients for tension, bending, and impact strength ( $R^2$ ) are 0.9846, 0.9836, and 0.9850.
- The weight proportion of the inclusion of TiO<sub>2</sub> additives is one of the greatest crucial elements, according to the RSM conclusion. Hybrid composites with improved mechanical properties result from the fusion of several elements. Since regulated fillers reinforce stability, the 4 wt% of TiO<sub>2</sub> demonstrated increased mechanical strength compared to 2 wt% and 6 wt%. ANN verifies this because 6 wt% filler creates accumulation, which reduces the mechanical properties of the composites.
- 200 gsm of Kevlar fiber provides maximum mechanical strength compared to 100 gsm. This is because a mat made of 200-gsm fiber requires greater force to separate the fiber bundles. Cryogenic therapy lasting 20 min rather than 10 and 30 min shows the greatest strength. The fiber and matrix have higher compatibility after 20 min of cryogenic treatment.
- The ANN also displays values of 0.9864 for impact strength, 0.9842 for flexural, and 0.9764 for tensile. ANN and RSM models were used to predict the mechanical efficiency of the suggested nanocomposites with up to 95% reliability. Depending on the results of mechanical qualities as opposed to the real, RSM and ANN are anticipated to be more dependable.

The study of cryogenic settings is particularly interesting because it provides insights into how hybrid composites behave when exposed to extreme temperature variations. The difficulties presented by cold temperatures highlight the significance of creating materials capable of preserving their firmness in these circumstances.

## 6 Application and future scope

The study's conclusions about the statistical techniques used to optimize TiO<sub>2</sub>-based interlaced Kevlar/epoxy hybrid composites have important ramifications for various applications. These improved lightweight materials exhibit superior mechanical qualities over and beyond those of their constituent parts. Advanced aircraft materials that can tolerate large temperature swings and provide hardness and endurance in challenging circumstances are examples of potential uses. These composite materials may also be used to create components with high strength and resistance appropriate for the automotive and military sectors. With precise weight ratios of TiO<sub>2</sub> and Kevlar fiber, the improved composite formula guarantees better performance and dependability, making it a potential option for applications where structural integrity is crucial. The study also points to possible applications in industries such as construction, where stronger mechanical properties are crucial. These results open the door to creating composite substances with various

uses in challenging situations, including aircraft and automobiles.

### 6.1 Future scope

- **Advanced material development:** The results offer a solid basis for further research into composite materials. Future studies might concentrate on customizing these materials for particular uses, such as lightweight and durable parts for the aerospace, automobile, and defense sectors. This may result in novel materials with even more remarkable qualities.
- **Environmental considerations:** Developing environmentally friendly composites has potential as people's awareness of ecological issues grows. Research into environmentally friendly matrices, fillers, and manufacturing methods may create green hybrids that satisfy performance and sustainability standards.
- **Smart composite materials:** The creation of smart materials may be made possible by incorporating sensors and monitoring features into such composites. In particular, these substances are important for monitoring structural health in civil and aeronautical engineering applications because they can give immediate information on their strength and damage.
- **Automation and industrial adoption:** Another interesting area is the industrial use of these sophisticated composites. It is possible to expedite the manufacturing process and increase its cost-effectiveness and accessibility for various applications using automation and optimization.
- **Cryogenic applications:** Additional investigation into the behavior of these hybrid composites in cryogenic environments can yield important information for space exploration, medical technology, and other sectors that deal with extremely low temperatures.
- **Predictive modeling:** The precision of forecasting mechanical characteristics can be improved by creating more complex forecasting algorithms, perhaps with the help of artificial intelligence and machine learning. This would simplify the creation of materials with particular characteristics for various purposes.
- **Cross-disciplinary collaborations:** Creative solutions can be discovered through collaboration involving researchers from other domains, engineers, and materials scientists. For instance, the medical sector may profit from these materials' strength, biocompatibility, and low weight to create implants and prosthetics.

The potential for innovation in a variety of sectors as well as the need for superior materials in various industries presents a large and attractive scope for advanced research in the field of hybrid materials.

### Data availability statement

The original contributions presented in the study are included in the article/Supplementary Material; further inquiries can be directed to the corresponding author.

## Author contributions

LN: conceptualization, methodology, resources, validation, and writing—original draft. GJ: data curation, formal analysis, methodology, and writing—review and editing. PP: supervision, visualization, and writing—review and editing. SD: project administration, resources, supervision, and writing—review and editing.

## Funding

The author(s) declare that no financial support was received for the research, authorship, and/or publication of this article.

## References

- Alsaadi, M., Uгла, A. A., and Erklig, A. (2017). A comparative study on the interlaminar shear strength of carbon, glass, and Kevlar fabric/epoxy laminates filled with SiC particles. *J. Compos. Mater.* 51 (20), 2835–2844. doi:10.1177/0021998317701559
- Behnam Hosseini, S. (2020). Natural fiber polymer nanocomposites. *Fiber-Reinforced Nanocomposites Fundam. Appl.*, 279–299. doi:10.1016/B978-0-12-819904-6.00013-X
- Chowdhury, M. A., Hossain, N., Shuvho, M. B. A., Kowser, M. A., Islam, M. A., Ali, M. R., et al. (2021). Improvement of interfacial adhesion performance of the kevlar fiber mat by depositing SiC/TiO<sub>2</sub>/Al<sub>2</sub>O<sub>3</sub>/graphene nanoparticles. *Arabian J. Chem.* 14 (11), 103406. doi:10.1016/j.arabj.2021.103406
- Deka, D. J., Sandeep, G., Chakraborty, D., and Dutta, A. (2005). Multiobjective optimization of laminated composites using finite element method and genetic algorithm. *J. Reinf. Plastics Compos.* 24 (3), 273–285. doi:10.1177/0731684405043555
- Devarajan, Y., Nagappan, B., Choubey, G., Vellaiyan, S., and Mehar, K. (2021). Renewable pathway and twin fueling approach on ignition analysis of a dual-fuelled compression ignition engine. *Energy and Fuels* 35 (12), 9930–9936. doi:10.1021/acs.energyfuels.0c04237
- Friedrich, K. (2018). Polymer composites for tribological applications. *Adv. Industrial Eng. Polym. Res.* 1 (1), 3–39. doi:10.1016/j.aiepr.2018.05.001
- Ganesan, V., and Kaliyamoorthy, B. (2020). Utilization of taguchi technique to enhance the interlaminar shear strength of wood dust filled woven jute fiber reinforced polyester composites in cryogenic environment. *J. Nat. Fibers* 19, 1990–2001. doi:10.1080/15440478.2020.1789021
- Hemanth, R. D., Kumar, M. S., Gopinath, A., and Natrayan, L. (2017). Evaluation of mechanical properties of E-Glass and coconut fiber reinforced with polyester and epoxy resin matrices. *Int. J. Mech. Prod. Eng. Res. Dev.* 7 (5), 13–20. doi:10.24247/ijmperdoct20172
- Hussain Syal, S., Ali Jogi, S., Muhammadi, S., Ahmed Laghari, Z., Ali Khichi, S., Naseem, K., et al. (2021). Mechanical characteristics and adhesion of glass-Kevlar hybrid composites by applying different ratios of epoxy in lamination. *Coatings* 11 (1), 94. doi:10.3390/coatings11010094
- Ismail, S. O., Akpan, E., and Dhakal, H. N. (2022). Review on natural plant fibres and their hybrid composites for structural applications: recent trends and future perspectives. *Compos. Part C. Open Access* 9, 100322. doi:10.1016/j.jcomc.2022.100322
- Jawaid, M., Chee, S. S., Asim, M., Saba, N., and Kalia, S. (2022). Sustainable kenaf/bamboo fibers/clay hybrid nanocomposites: properties, environmental aspects and applications. *J. Clean. Prod.* 330, 129938. doi:10.1016/j.jclepro.2021.129938
- Kara, M., Kırıcı, M., Tatar, A. C., and Avci, A. (2018). Impact behavior of carbon fiber/epoxy composite tubes reinforced with multi-walled carbon nanotubes at cryogenic environment. *Compos. Part B Eng.* 145, 145–154. doi:10.1016/j.compositesb.2018.03.027
- Li, Y., Mai, Y. W., and Ye, L. (2000). Sisal fibre and its composites: a review of recent developments. *Compos. Sci. Technol.* 60, 2037–2055. doi:10.1016/S0266-3538(00)00101-9
- Li, Z., Wang, X., and Wang, L. (2006). Properties of hemp fibre reinforced concrete composites. *Compos. Part A Appl. Sci. Manuf.* 37, 497–505. doi:10.1016/j.compositesa.2005.01.032
- Luzi, F., Puglia, D., and Torre, L. (2019). 10 - natural fiber biodegradable composites and nanocomposites: a biomedical application. *Biomass, Biopolymer-Based Mater. Bioenergy Constr. Biomed. Other Industrial Appl.*, 179–201. doi:10.1016/B978-0-08-102426-3.00010-2

## Conflict of interest

The authors declare that the research was conducted in the absence of any commercial or financial relationships that could be construed as a potential conflict of interest.

## Publisher's note

All claims expressed in this article are solely those of the authors and do not necessarily represent those of their affiliated organizations, or those of the publisher, the editors, and the reviewers. Any product that may be evaluated in this article, or claim that may be made by its manufacturer, is not guaranteed or endorsed by the publisher.

Maharana, S. M., Pandit, M. K., and Pradhan, A. K. (2021). Influence of fumed silica nanofiller and stacking sequence on interlaminar fracture behaviour of bidirectional jute-kevlar hybrid nanocomposite. *Polym. Test.* 93, 106898. doi:10.1016/j.polymeresting.2020.106898

Mannan, K. T., Sivaprakash, V., Raja, S., Patil, P. P., Kaliappan, S., and Socrates, S. (2022). Effect of Roselle and biochar reinforced natural fiber composites for construction applications in cryogenic environment. *Mater. Today Proc.* 69, 1361–1368. doi:10.1016/j.matpr.2022.09.003

Matykiewicz, D. (2020). Hybrid epoxy composites with both powder and fiber filler: a review of mechanical and thermomechanical properties. *Materials* 13 (8), 1802. doi:10.3390/ma13081802

Mohit, H., Rangappa, S. M., Gapsari, F., Siengchin, S., Marwani, H. M., Khan, A., et al. (2023). Effect of bio-fibers and inorganic fillers reinforcement on mechanical and thermal characteristics on carbon-kevlar-basalt-innegra fiber bio/synthetic epoxy hybrid composites. *J. Mater. Res. Technol.* 23, 5440–5458. doi:10.1016/j.jmrt.2023.02.162

Nayak, S., Nayak, R. K., and Panigrahi, I. (2022). Effect of nano-fillers on low-velocity impact properties of synthetic and natural fibre reinforced polymer composites—a review. *Adv. Mater. Process. Technol.* 8 (3), 2963–2986. doi:10.1080/2374068x.2021.1945293

Pragadish, N., Kaliappan, S., Subramanian, M., Natrayan, L., Satish Prakash, K., Subbiah, R., et al. (2022). Optimization of cardanol oil dielectric-activated EDM process parameters in machining of silicon steel. *Biomass Convers. Biorefinery* 14, 121–135. doi:10.1007/s13399-021-02268-1

Prasob, P. A., and Sasikumar, M. (2018). Static and dynamic behavior of jute/epoxy composites with ZnO and TiO<sub>2</sub> fillers at different temperature conditions. *Polym. Test.* 69, 52–62. doi:10.1016/j.polymertesting.2018.04.040

Prasob, P. A., and Sasikumar, M. (2019). Viscoelastic and mechanical behaviour of reduced graphene oxide and zirconium dioxide filled jute/epoxy composites at different temperature conditions. *Mater. Today Commun.* 19, 252–261. doi:10.1016/j.mtcomm.2019.02.005

Praveenkumara, J., Madhu, P., Yashas Gowda, T. G., Sanjay, M. R., and Siengchin, S. (2022). A comprehensive review on the effect of synthetic filler materials on fiber-reinforced hybrid polymer composites. *J. Text. Inst.* 113 (7), 1231–1239. doi:10.1080/00405000.2021.1920151

Ramesh, C., Vijayakumar, M., Alshahrani, S., Navaneethkrishnan, G., Palanisamy, R., Natrayan, L., et al. (2022). Performance enhancement of selective layer coated on solar absorber panel with reflector for water heater by response surface method: a case study. *Case Stud. Therm. Eng.* 36, 102093. doi:10.1016/j.csite.2022.102093

Rana, A. K., Mandal, A., Mitra, B. C., Jacobson, R., Rowell, R., and Banerjee, A. N. (1998). Short jute fiber-reinforced polypropylene composites: effect of compatibilizer. *J. Appl. Polym. Sci.* 69, 329–338. doi:10.1002/(sici)1097-4628(19980711)69:2<329::aid-app14>3.0.co;2-r

Sabarinathan, P., Annamalai, V. E., Vishal, K., Nitin, M., Natrayan, L., Veeeman, D., et al. (2022). Experimental study on removal of phenol formaldehyde resin coating from the abrasive disc and preparation of abrasive disc for polishing application. *Adv. Mater. Sci. Eng.* 2022, 1–8. doi:10.1155/2022/6123160

Santhosh, M. S., Sasikumar, R., Natrayan, L., Kumar, M. S., Elango, V., and Vanmathi, M. (2018). Investigation of mechanical and electrical properties of Kevlar/E-glass and Basalt/E-glass reinforced hybrid composites. *Int. J. Mech. Prod. Eng. Res. Dev.* 8 (3), 591–598. doi:10.24247/ijmperdjun201863

Sethi, S., Rathore, D. K., and Ray, B. C. (2015). Effects of temperature and loading speed on interface-dominated strength in fibre/polymer composites: an evaluation for *in-situ* environment. *Mater. Des. (1980-2015)* 65, 617–626. doi:10.1016/j.matdes.2014.09.053

- Su, F. H., Zhang, Z. Z., and Liu, W. M. (2008). Tribological behavior of hybrid glass/PTFE fabric composites with phenolic resin binder and nano-TiO<sub>2</sub> filler. *Wear* 264, 562–570. doi:10.1016/j.wear.2007.04.007
- Thakur, V. K., Thakur, M. K., and Gupta, R. K. (2014). Review: raw natural fiber-based polymer composites. *Int. J. Polym. Analysis Charact.* 19, 256–271. doi:10.1080/1023666X.2014.880016
- Uma Devi, L., Bhagawan, S. S., and Thomas, S. (1997). Mechanical properties of pineapple leaf fiber-reinforced polyester composites. *J. Appl. Polym. Sci.* 64, 1739–1748. doi:10.1002/(sici)1097-4628(19970531)64:9<1739::aid-app10>3.0.co;2-t
- Velmurugan, G., and Babu, K. (2020). Statistical analysis of mechanical properties of wood dust filled Jute fiber based hybrid composites under cryogenic atmosphere using Grey-Taguchi method. *Mater. Res. Express* 7, 065310. doi:10.1088/2053-1591/ab9ce9
- Velmurugan, G., and Natrayan, L. (2023). Experimental investigations of moisture diffusion and mechanical properties of interply rearrangement of glass/Kevlar-based hybrid composites under cryogenic environment. *J. Mater. Res. Technol.* 23, 4513–4526. doi:10.1016/j.jmrt.2023.02.089
- Velmurugan, G., Natrayan, L., Chohan, J. S., Vasanthi, P., Angalaeswari, S., Pravin, P., et al. (2023). Investigation of mechanical and dynamic mechanical analysis of bamboo/olive tree leaves powder-based hybrid composites under cryogenic conditions. *Biomass Convers. Biorefinery* 14, 1–13. doi:10.1007/s13399-023-04591-1
- Xu, F., Fan, W., Zhang, Y., Gao, Y., Jia, Z., Qiu, Y., et al. (2017). Modification of tensile, wear and interfacial properties of Kevlar fibers under cryogenic treatment. *Compos. Part B Eng.* 116, 398–405. doi:10.1016/j.compositesb.2016.10.082
- Yıldırım, F., Tatar, A. C., Eskizeybek, V., Avci, A., and Aydın, M. (2021). Impact response of nanoparticle reinforced 3D woven spacer/epoxy composites at cryogenic temperatures. *J. Compos. Mater.* 55 (28), 4231–4244. doi:10.1177/00219983211037052
- Yogesh, P., Singarayar, S. P., Rajkamal, M. D., Venkatesh, T., kumar Gupta, R., and Yatika, G. (2022). Mechanical performance of aloe vera/dharbai-based hybrid epoxy composites with enhanced NaHCO<sub>3</sub> treatment. *Mater. Today Proc.* 69, 1394–1401. doi:10.1016/j.matpr.2022.09.204
- Zhang, Z. Z., Zhang, H. J., Guo, F., Wang, K., and Jiang, W. (2009). Enhanced wear resistance of hybrid PTFE/Kevlar fabric/phenolic composite by cryogenic treatment. *J. Mater. Sci.* 44, 6199–6205. doi:10.1007/s10853-009-3862-4